IIETA International Information and Engineering Technology Association
Advancing the World of Information and Engineering

Mathematical Modelling of Engineering Problems
Vol. 11, No. 5, May, 2024, pp. 1160-1170
Journal homepage: http://iieta.org/journals/mmep

Artificial Intelligence for Mechanical Properties Prediction of Polyethylene-Carbon Nanotube Composites

Carlos Serrano[1], Nestor Ulloa[1,2*], Christian Flores[1], Fausto Caicedo[1]

[1] Facultad de Mecánica, Escuela Superior Politécnica de Chimborazo (ESPOCH), Riobamba 060155, Ecuador
[2] Grupo de Investigación y Desarrollo de Nanotecnología, Materiales y Manufactura (GIDENM), Escuela Superior Politécnica de Chimborazo (ESPOCH), Riobamba 060155, Ecuador

Corresponding Author Email: nestor.ulloa@espoch.edu.ec

https://doi.org/10.18280/mmep.110504

Received: 17 November 2023
Revised: 22 January 2024
Accepted: 30 January 2024
Available online: 30 May 2024

Keywords:
artificial intelligence, carbon nanotubes, depth sending indentation, elastic modulus, mechanical performance, polyethylene

ABSTRACT

The novel class of composite materials known as polyethylene-carbon nanotube composites (PECNTs) has attracted significant interest from scientists. In this study, authors investigated how artificial intelligence (AI) is employed to calculate the elastic modulus of PECNTs. For the first time, an AI-based modeling methodology replaces nanoindentation techniques like depth sensing indentation (DSI). This study highlights the complexities inherent in traditional methods, where the proposed methodology utilizes a gene expression programming (GEP) model, addressing challenges associated with accuracy in PECNT simulation. The proposed AI model test uses 135 input/output data pairs taken from the literature and randomly split into 82 training and 53 testing sets. The elastic modulus (EM) whichever dynamic E′ or quasi-static E) employs as an output factor in the models created, with the method of analysis, matrix type, processing technique, nanofiller type, and its content serving as inputs. Though the modeling progression is complete with results from the training and testing sets, the nanometer sensitivity of the prominent designs of the AI model displayed significant promise for the effective application of artificial intelligence methods in measuring the elastic modulus of PECNTs through non-destructive testing.

1. INTRODUCTION

Depth sensing indentation (DSI) stands out as an essential mechanical method for material characterization [1]. The dynamic surface indentation (DSI) technique meticulously measures and records the depths of indentation and retraction of a penetrator while applying and removing a load on a standard material [2, 3]. The approach known as "nanoindentation" leverages DSI at a penetration depth of just a few microns [4, 5]. The DSI testing process involves distinct phases: loading, holding, and unloading, as illustrated (Figure 1). The analysis of the load-depth curve is carried out using elastic contact principles [6]. Estimating the quasi-static elastic modulus E is feasible due to the linear elastic behavior at the beginning of the unloading phase [7-9]. Instrumented indentation, by applying minimal focused deformation, facilitates the study of the material's mechanical properties [10]. Although limited research systems exist, particularly those with highly restricted parameters, can be beneficial, as in the case of thin films and coatings [11, 12]. However, DSI goes beyond by offering the capability to spatially resolve mechanical characteristics in heterogeneous materials, providing additional benefits, as seen in the case of polyethylene nanocomposites.

The incorporation of nanofillers into polyethylene materials yields a significant advantage in optical, electrical, mechanical, thermal, and fire-retardant qualities [13, 14]. These properties make such materials particularly useful in sectors such as electronics, automobiles, and aviation. Specifically, carbon nanotubes (CNTs) have attracted considerable interest as a potentially optimal nanofiller for polyethylene due to their exceptional electrical and mechanical characteristics [15, 16]. In this context, depth-sensing indentation emerges as the method of choice for evaluating the mechanical factors of polyethylene materials, thanks to its higher signal accuracy and examination of reduced material volumes [17-19]. However, to further optimize its utility, it is essential to emphasize the need for a smoother transition in the narrative, especially when transitioning from the discussion of DSI to exploring the potential of carbon nanotubes in polyethylene composites [20]. This improvement in narrative coherence and flow will help effectively contextualize the importance of artificial intelligence (AI) in enhancing the current limitations of DSI, providing a clearer and more comprehensive view of the presented research [21, 22].

Mechanical and physical characteristics of material are evaluated with the help of several AI-based methods, such as ANN and GEP [23, 24]. For many GEP models, projecting forward from current conditions is the ultimate goal [25, 26]. It's essential to consider the impact of input and output variables and product quality early in the process planning phase [27-29].

The GEP has several benefits but infrequently engages in the pitch of science materials [30, 31]. Applications of GEP in materials engineering range from predicting the synthesis time of materials to modeling binding strength in polyethylene to simulating the hardness of nanocomposites. The current work showed polyethylene-carbon nanotube composites' elastic module properties using GEP (PECNTs) [32]. The term "nanoindentation" has never before applying to a simulation [33, 34]. Across a suitable scope, this study introduced a safe approach to ascertain the elastic modulus (quasi-static) of polyethylene-carbon nanotube composites. The model outcomes suggest that the proposed method could serve as a viable substitute for the depth sensing indentation technique.

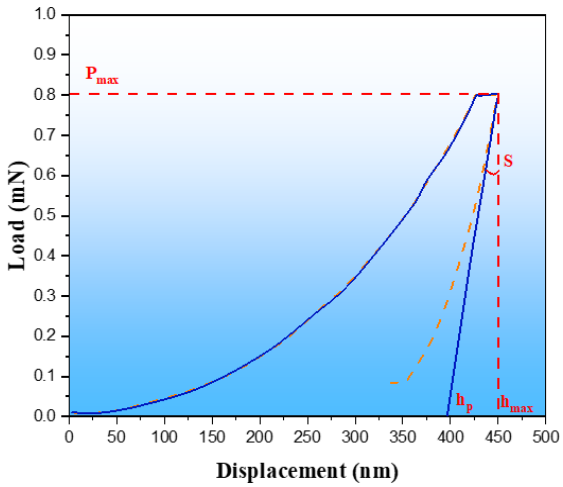

Figure 1. The load exerted on a semi-crystalline PEEK specimen versus indentation depth (degree of crystallinity of 40%)

2. METHODS AND MATERIALS

2.1 AI in properties of composite materials

Recent progress in the use of artificial intelligence (AI) techniques has highlighted the significance of traditional machine learning (ML) and deep learning (DL) approaches for the prediction of composite materials' mechanical properties. These approaches have been effectively used to predict critical mechanical properties accurately. However, their success largely hinges on data availability and the efficiency of the learning models [35]. The performance of composite materials can be greatly affected by their microstructure and composition. While most existing techniques focus on predicting properties based on either microstructure or material components, there is often a lack of comprehensive data utilization. This challenge has prompted the creation of a new multimodal material performance prediction model that incorporates a network for extracting features from material microstructures [36].

2.2 Analysis of method

The elastic modulus derived from the methods often used to interpret load-depth data from DSI is highly accurate. In this work, authors have included the most crucial of these approaches as input parameters in the model—the model developed by Oliver and Pharr. Following the above inspections and measurements, a plot of applying load vs. penetration depth attain from a rough force curve. The following equation describes the relationship between the methodology, reduced modulus (Er), contact stiffness (S) as well as the predicted contact area (A):

$$E_r = \frac{\sqrt{\pi}}{2\beta}\frac{S}{\sqrt{A}} \tag{1}$$

where,

$$\frac{1}{E_r} = \frac{(1-v^2)}{E} + \frac{(1-v_i^2)}{E_i} \tag{2}$$

E: elastic modulus f the material
v: Poisson's ratio of the material
E_i: indenter of elastic modulus
v_i: indenter of Poisson's ratio

The Oliver and Pharr method overestimates the contact area and underestimates the modulus of elasticity when used to pileup materials (where the pile-up is constrained) [37].

2.3 Dynamic strategy

As an alternate method for investigating the time-dependent behavior of polyethylene, dynamic indentation testing (or continuous stiffness measurements, CSM) offers exact results. During a dynamic indentation test, the quasi-static loading profile encloses an additional cycle (sinusoidal oscillation). Throughout the tests, the contact stiffness determines by measuring the amplitude of load, displacement, and phase lag among them. During a dynamic test, stiffness is a constant. The Hertz contact model is employed to illustrate the storage modulus (E') and loss modulus (E"), determined by the ratio of the applied force to the adhesion force [38]. This technique called nano dynamic mechanical analysis (nano DMA), has recently been brought to the marketplace. Specifically, the complex modulus of a viscoelastic material is:

$$E^* = E' + iE'' \tag{3}$$

whereas,

$$E' = E\cos\,\delta \tag{4}$$

and,

$$E'' = E\sin\,\delta \tag{5}$$

δ: phase shifts among the complex
E: standard quasi-static modulus

There is no distinction between quasi-static and dynamic indentation moduli in the DSI literature.

2.4 Polyethylene-carbon nanotube composites

Carbon nanotubes are one of the most valuable nanofillers (CNT) to enhance polyethylene matrix. CNTs split into two distinct varieties. The initial type, known as single-walled carbon nanotubes (SWCNTs), consists of a single graphene sheet wrapped into a cylindrical tube with a diameter ranging from 0.7 to 3 nm. Figure 2 depicts a multi-walled carbon nanotube (MWCNT), which consists of more than two coaxial cylinders made from single sheets and has a diameter ranging from 2 to 40 nm. CNTs produced through diverse techniques such as arc discharge, laser ablation, and chemical vapor

deposition, hydrothermal synthesis, electrolysis, and the solar process [39, 40]. The results of these multiple approaches vary significantly in terms of their purity and quality. Therefore, the "nanofiller type" can be employed as a second model parameter.

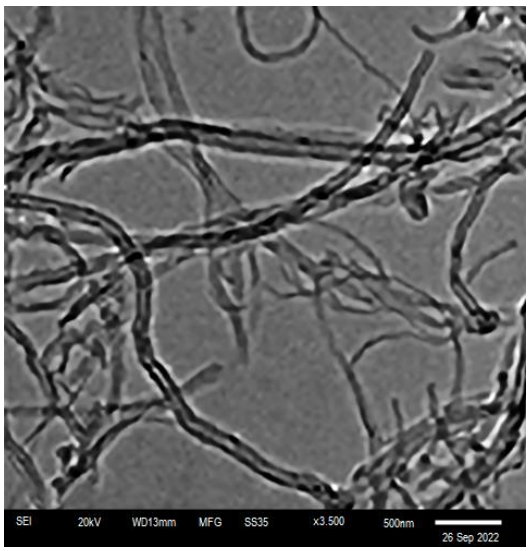

Figure 2. Transmission electron microscopic of carbon nanotubes

Nanocomposites created by combining polyethylene and carbon nanotubes. To complete the process, the model needs to consider the production process for polyethylene-carbon nanotube composites [41, 42]. One of the biggest challenges in developing and using filled polyethylene is getting a uniform distribution of Carbon Nanotubes in the matrix by eliminating the Vander Waals interface among the individual tubes [43, 44]. Due to their high aspect ratio and non-Brownian nature, CNTs are not distributed uniformly in a polyethylene matrix. The reinforcing CNTs' inability to transfer loads efficiently across the CNT/matrix interface is mixed because they are passive and can only contact the matrix around them through van der Waals forces. Various methods, such as mechanical dispersion techniques like ultrasonication, ball-milling, plasma treatment, and chemical modification, are employed to address these two challenges. Pulverization, densification, and coagulant spinning are projects for preparing polyethylene/CNT nanocomposites. Milling; Melt blending; in situ polyethyleneization; and latex technology.

2.5 Gene expression programming theory

Genetic programming (GP), which draws inspiration from Darwin's idea of natural selection, is a rapidly expanding subfield of evolutionary algorithms [45]. It is a subfield of supervised machine learning that examines existing code instead of looking at data.

GP used the following three methods for developing software that solves problems:

(1). Repeat the following stage still the final condition attains.

(2). Create a random sample of computer programs with the problem's primitive functions and terminals.

a) Run each stubborn population to attain a fitness portion that indicates the quality in which the software solves the problem.

b) Generate a fresh set of programs by applying the following fundamental manipulations to a subset of the original location of programs with selection probabilities determined by fitness.

(i) Reproduce: implement a previously tested method in the new population.

(ii) New software develops by combining existing programs or "crossing them over," as the linguists.

(iii) It is possible to generate novel software through mutation.

(iv) Select a program for which would like to perform an operation that would change its underlying architecture.

(3). The best database from the population created throughout the run is identified as the product of genetic programming.

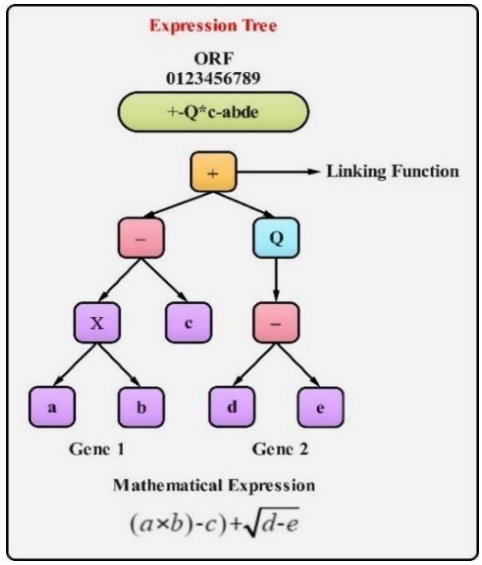

Figure 3. Expression tree and accompanying mathematical equation for a chromosome containing two genes

Evolutionary algorithms based on populations are called gene expression programming (GEP). People in GEP view them as either non-linear entities of varying sizes and forms or linear strings of a constant length (genome). Authors refer to these things as "expression trees" (ETs) [46, 47]. Each person has a single chromosome, and each gene on any given chromosome divides between the chromosome's head and tail. Genetic expression transcripts (ETs) are selected based on their fitness value to produce offspring.

Consider the algebraic statement $[(b \times a) - c)] + \sqrt{(d - e)}]$. Figure 3 shows that a language with a linguistic basis in ETs classified as having either a chromosome with only two genes or an ET.

2.6 AI model

Gene expression programming (GEP) theory represents a powerful methodology in the field of artificial intelligence. This theory is based on principles inspired by genetics and evolution to create robust predictive models. In the design of a model using GEP, genetic program structures are employed that evolve and adapt over time. These programs, expressed in the form of expression trees, capture the complexity of genetic interactions and allow for modeling complex phenomena. GEP theory has been successfully used in predicting the mechanical properties of composite materials, highlighting its

ability to address complex problems and extract meaningful patterns from data.

2.7 Data selection

Table 1 presents the compiled information from the preceding works. In this investigation, a Gene Expression Programming (GEP) model was employed to predict the elastic modulus of polyethylene-CNT composites, serving as the primary objective or cost function [48]. The possible values for the input factors are listed in Table 2. Further details regarding the results shown in Table 1 can be found in Table 3. For instance, "Raw MWCNTs" would be listed as the first option under "nanofiller type" (1).

Table 1. The collected data serves as input and target for training and testing sets obtained from previous studies

Matrix Type	Kinds of Nanofi	Processing Techni	Content of Nanofiller (wt%)	Analysis Method	DSI Modul US (GPa)	Ref.
1	1	1	0	1	1.81	[1]
1	1	1	0.25	1	2.2	[1]
1	1	1	0.75	1	2.6	[1]
1	1	1	0	1	2.2	[1]
1	1	1	0.25	1	2.5	[1]
1	1	1	0.75	1	2.05	[2, 7]
2	9	2	0	3	3.9	[1]
2	9	2	0.1	3	3.78	[7]
2	9	2	0.5	3	3.98	[1]
2	9	2	1	3	4.06	[7]
2	9	2	3	3	4.25	[1]
2	9	2	5	3	4.56	[7]
2	2	2	0	2	4.22	[1]
2	2	2	0.1	2	4.7	[7]
2	2	2	0	2	4.53	[1]
2	2	2	3	2	4.75	[7]
2	1	2	0	2	3.16	[13, 48]
2	1	2	0.1	2	3.19	[13, 48]
2	1	2	0.5	2	3.35	[36]
2	1	2	1	2	3.44	[36]
2	2	3	0	3	3.7	[32]
2	2	3	5	3	7.4	[32]
2	2	4	0	2	2.26	[32]
2	2	4	1	2	3.1	[16]
2	2	4	2	2	3.64	[16]
2	1	5	0	2	3	[27, 28]
2	1	5	1	2	3	[27, 28]
2	4	3	0	3	3.7	[27, 28]
2	4	3	5	3	7.55	[27, 28]
2	4	3	5	3	4.25	[27, 28]
2	5	5	0	2	3	[27, 28]
2	5	5	1	2	3	[27, 28]
2	6	5	0	2	3	[27, 28]
2	6	5	1	2	3	[24]
2	7	3	0	2	4.22	[24]
2	8	6	0	2	4	[24]
2	8	6	1	2	4.4	[24]
2	8	6	3	2	5.6	[11]
2	8	6	0	3	4	[12]
2	8	6	1	3	5	[18]
2	8	6	3	3	5.9	[18]
2	10	7	0	1	3.6	[18]
2	10	7	0.5	1	4	[18]
2	10	8	0	2	3.6	[18]
2	10	9	0.75	2	4.8	[18]
2	10	9	5.5	2	4.9	[26]
2	10	9	14.2	2	6	[26, 31]
2	10	9	14.2	2	8.8	[43]
2	11	10	0	2	4.8	[43]
2	11	10	0.75	2	4.6	[43]
2	11	10	3	2	5.1	[43]
2	12	2	0	2	4.9	[43]
2	12	2	1	2	5.6	[43]
2	12	2	3	2	6	[43]
2	12	2	5	2	7	[33]
2	13	11	0	2	2.23	[33]
3	14	12	0	2	5.66	[33]
3	14	12	1	2	7.62	[33]

3	14	12	10	2	11.74	[34]
4	15	13	0	3	2.3	[46]
4	15	13	0.1	3	2.6	[46]
4	15	13	0.2	3	3.15	[46]
4	15	13	0.5	3	3.5	[41]
5	14	12	0	2	0.12	[46]
5	14	12	1	2	0.15	[46]
5	14	12	10	2	0.53	[46]
6	1	14	0	2	1.45	[46]
6	1	14	0.4	2	2.22	[46]
6	1	14	1	2	2.23	[46]
6	1	14	1.3	2	1.58	[14]
6	1	14	1.6	2	2.64	[14]
6	1	14	2.2	2	2.02	[14]
6	1	14	2.4	2	2	[14]
7	16	15	0	3	1.18	[14]
7	16	15	0.2	3	1.33	[14]
7	16	15	0.5	3	1.6	[14]
7	16	15	1	3	2.02	[20]
7	17	16	0	2	0.95	[20]
7	17	16	1	2	1.56	[20]
7	17	16	2.5	2	2.14	[20]
7	17	16	5	2	2.38	[23]
7	17	16	7.5	2	2.66	[23]
8	18	17	0	2	3.6	[23]
8	18	17	1.25	2	4.4	[23]
8	18	17	2.5	2	5.8	[23]
8	18	17	3.75	2	6.6	[39]
8	18	17	5	2	7.5	[39]
8	18	17	6.25	2	7.8	[39]
9	1	18	0	2	2.02	[39]
9	1	18	0.5	2	2.23	[39]
9	19	13	0	3	2.75	[41, 42]
9	19	13	0.05	3	3.1	[38]
9	19	13	0.1	3	4.26	[46]
9	19	13	0.2	3	4.35	[46]
9	17	19	0	2	0.617	[46]
9	17	19	0.5	2	0.728	[46]
9	17	19	1	2	0.808	[41]
9	17	19	1.5	2	0.925	[41]
9	17	19	2	2	1.67	[41]
9	17	19	2.5	2	1.75	[41]
9	17	19	5	2	1.89	[41]
10	1	20	0	1	0.26	[41]
10	1	20	0.3	1	0.31	[41]
11	20	21	0	1	7	[24]
11	20	21	0.25	1	9.4	[29]
11	20	21	0.5	1	10.4	[29]
11	21	12	0	2	0.66	[29]
11	21	12	0.2	2	6.93	[29]
11	21	12	0.4	2	7.3	[33]
11	21	12	0.6	2	7.8	[33]
12	22	22	0	3	3.9	[33]
12	22	22	1	3	4.25	[33]
12	23	22	0	3	3.9	[23]
12	23	22	1	3	4.6	[23]
13	1	23	0	2	0.0067	[23]
13	1	23	4	2	0.0089	[23]
14	2	24	0	2	4	[23]
14	2	24	2	2	4.2	[23]
14	2	24	4	2	4.4	[18]
14	2	24	6	2	4.5	[18]
14	2	24	15	2	5.2	[18]
15	24	25	0	3	5.23	[18]
15	24	25	0.5	3	8.41	[18]
16	20	21	0	1	2	[44]
16	20	21	0.5	1	2.24	[44]
16	20	21	1	1	3.1	[29]
16	20	21	2	1	2.56	[29]
16	20	21	4	1	2.96	[29]
16	20	21	8	1	6	[29]

17	25	26	0	2	3.6	[29]
17	25	26	1	2	3.38	[29]
17	25	26	3	2	3.67	[42, 44]
17	25	26	5	2	3.53	[42, 44]
17	25	26	2	2	3.48	[42, 44]
17	25	26	4	2	3.73	[42]

Table 2. The variety of input and output factors in the GEP model

Input	Output
Nanofiller type	1-25
Processing method	1-26
Nanofiller content (wt %)	0-15
Method of analysis	1-3
Type of Matrix	1-17

Table 3. Methods and raw materials used in previous studies

Symbol	Matrix Type	Nanofiller Type	Processing Method	Method of Analysis
1	Epoxyacrylate	Raw MWCNTs	Sonication/mixing photocuring	Non-available
2	Epoxy	CVD raw MWCNTs	Sonication/mixing curing in the oven	From unloading (OP)
3	Poly(3-hydroxybutyrate)	Raw CVD MWCNTs	Stirring/ mixing curing in the oven	Dynamic
4	Chitosan	Acid-functionalized CVD MWCNTs	Stirring/ mixing curing in a hot press	-
5	Poly(3-hydroxyoctanoate)	Fluorinated-SWCNTs	Stirring/ mixing curing in the oven	-
6	Polypropylene	Silane functionalized SWCNTs	Solution mixing curing in the oven	
7	Polyamide-6	Plasma functionalized CVD MWCNTs	Mixing/ Curing	
8	Poly (L-lactic acid)	MBZ functionalized Arc-discharge SWCNTs	In situ wetting/Realign/curing	
9	Ultra-high molecular weight polyethylene	Purified laser-grown SWCNTs	Mechanical densification/capillary-induced wet-ting/curing	
10	Polyvinylidene fluoride	Aligned CVDMWCNT forests	Shearmixing/curing	
11	Polyvinyl alcohol	NT forests CVDMWCNT forests	Curing	
12	Poly (ether ketone)/GF	Coiled CVDCNTs	Solution-casting	
13	Polydimenthylsiloxane	CVDCNTs grafted silica fiber	Solution mixing/casting	
14	PC	RawSWCNTs	In-situpolyethyleneization compression-molding	
15	Polyimide; PLLA: poly (L-lactic acid)	PEDOT-PSS functionalized	Melt-bending/compression molding	
16	Poly (9-vinyl carbazole)	Acid purifiedCVDMWCNTs	Solution mixing/electro spinnig	
17	Poly (methyl methacrylate)	Acid-functionalized MWCNTs	Sonication/solution-casting	
18		Acid-purified Arc-discharge MWCNTs	Milling/electrostatic spraying	
19		Plasma functionalized Arc discharge SWCNTs	Ball milling/compression molding	
20		Raw arc-discharge MWCNTs	Near-field electrospinning Solution mixing	
21		Acid functionalized Arc-discharge SWCNTs		
22		Arc purified SWCNTs	Melt-blending/ hot compression	
23		PEES-wrapped Arc-purified SWCNTs	Ultrasonication/curing	
24			Melt-extrusion	
25		Raw Arc-discharge SWCNTs	Sonication/spin-coating	
26		Amide-functionalized CVD MWCNTs	Solution mixing/spin coating	

3. RESULTS AND DISCUSSION

3.1 Process parameters and GEP

The initial step involves selecting the fitness function for the formulations based on gene expression programming (GEP). First, in Eq. (6), authors may determine the "f_i" equation as follows:

$$f_i = \sum_{j=1}^{C_i} \left(M - \left|C_{(i,j)} - T_j\right|\right) \quad (6)$$

whereas,

i is fitness case.

$C_{(i,j)}$ is return value.

j is out of CT. fitness cases.

T_j is the target value to fitness case *j*.

M is selection range.

One benefit of these fitness functions is that allow the structure to discover the best course of action on its own. The GEP model comprises six input layers, namely the matrix type (d0), nanofiller type (d1), processing technique (d2), nanofiller content (d3), and method of analysis (d4). The output layer is characterized by the application of the elastic modulus (either quasi-static E or dynamic, E′). The models listed in Table 1 incorporate a range of input parameters.

Figure 4 shows the expression trees generated by the GEP method developed in this study for predicting the values of the elastic modulus (EM) of PECNTs. Within this diagram, d0, d1, d2, d3, and d4 correspond to the aforementioned input layers. Specifically, d0 represents the matrix type, d1 signifies the type of nanofiller, d2 denotes the processing method, d3 indicates the nanofiller content, and d4 represents the analysis method.

A total of 135 experimental sets became rid of the literature; 82 selects for the training phase, and the remaining 53 sites went through their paces in the testing phase. Genetic evolution used the training data as its input. Elastic modulus was determined by evaluating GEP's best model against data not used in the initial model generation. The model with the highest EM on the practicing and experimenting value sets is selected based on these evaluations.

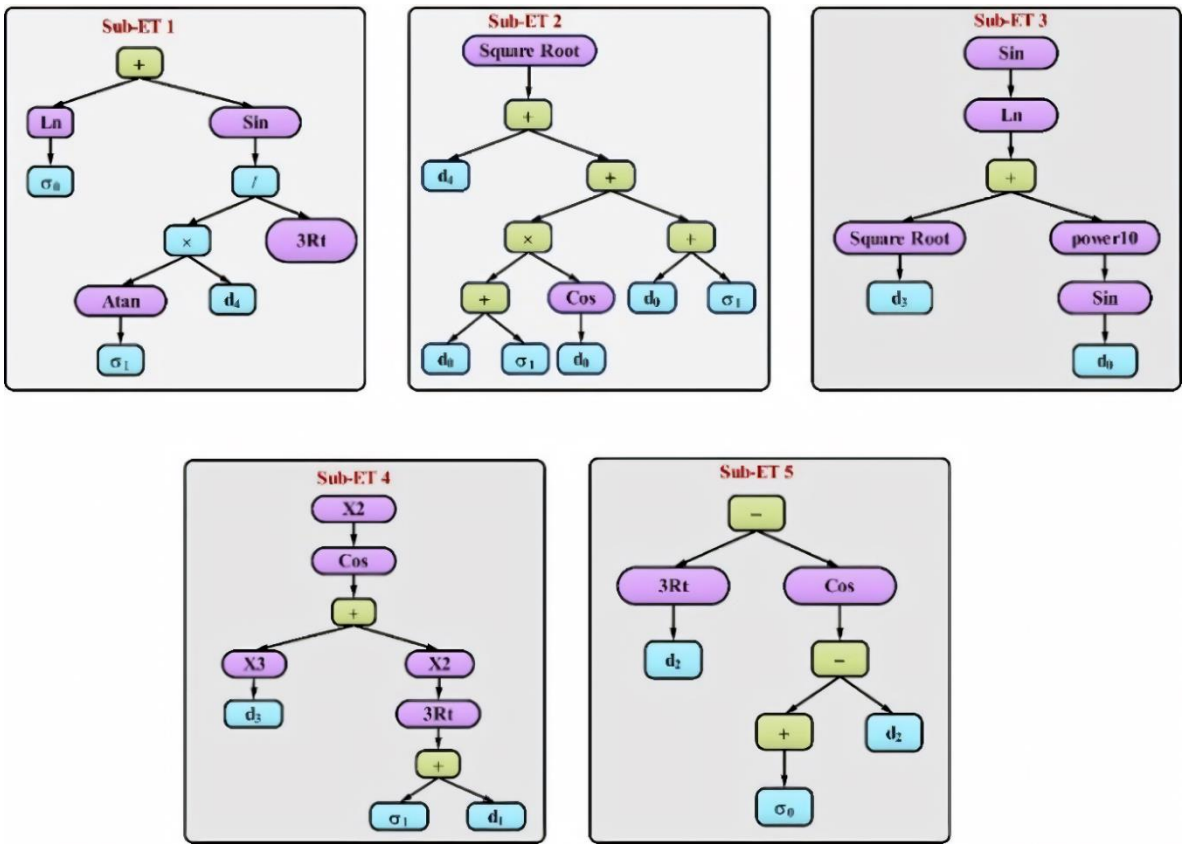

Figure 4. Predicting the elastic modulus of PECNTs using an expression tree including five genes

Table 4. Factors of the GEP approach model

Factor Definition	Values
Gene transposition rate	0.1
Chromosomes	30
Weight of functions	7
Head size	10
Inversion rate	0.1
Number of genes	5
Linking function	Multiplication
Gene recombination rate	0.1
Mutation rate	0.044
One-point recombination rate	0.3
Two-point recombination rate	0.3
Lower bound	10
Upper bound	10
Constants per gene	5

All modeling methodologies strive to accurately predict the target parameter in the output layer, whether by maximizing the root mean square error (RMSE) or minimizing the absolute percentage error (MAPE). Only if four genes are employed, and the connecting function employs multiplication, will these conditions be satisfied (x). It reveals that 30 chromosomes were present in the most predictive cohort for the elastic module. The GEP values that determine for this study are in Table 4.

As the second stage in chromosome construction, the pivotal task is to choose the set of terminals (T) and the set of functions (F). In this instance, the terminal set comprises the independent variables: Elastic modulus value = d0, d1, d2, d3, d4.

Some elementary functions (ln, sin, cos, Arctan, Exp, $\sqrt{x^2}, x^3,$) and the four elementary operators (+), (-), (x), and (/) are measured because selecting the best function set can be challenging for modeling. For f_s, an explicit model based on the GEP technique was used to obtain a formulation.

$$EMV = f\{d0, d1, d2, d3, d4\} \quad (7)$$

It is crucial to describe the principles for evaluating the results of the model, which are the model's performance and the accuracy of its predictions. The model's efficacy calculates across a variety of statistical scales. Comparing experimental (target) and predicted values, we employed criteria such as root-mean-squared error (RMSE), R-squared (R^2), and mean absolute error (MAE).

$$MAE = \frac{1}{n}\left[\frac{\sum_{i=1}^{n} |t_i - o_i|}{\sum_{i=1}^{n} t_i}\right] \quad (8)$$

$$RMSE = \sqrt{\frac{1}{n}\sum_{i=1}^{n} (t_i - o_i)^2} \quad (9)$$

$$R^2 = \frac{(n\sum t_i o_i - \sum t_i \sum o_i)^2}{(n\sum t_i^2 - (\sum t_i)^2)(n\sum o_i^2 - (\sum o_i)^2)} \quad (10)$$

whereas, (t, o, n) denotes the experimented range, the anticipated range, and the total no of data points, respectively. The Root means square statistic indicates how close the model results are to the experimental (target) results; a smaller value indicates an adjacent fit. If the Root Means Square statistical range is extensive, however, the outcome provided by the models diverges significantly from the experimented (target) values.

Eq. (11) follows from Figure 4 and is related to the GEP model.

$$EMV = \left(\ln 2.1 + \sin\left(\frac{(d_4 \times \arctan 3.73)}{\sqrt[3]{d_2}}\right)\right)x \sqrt{d_4 + \left((d_0 + 1.11) \times \cos d_0\right) + d_0 - 1.11\Big)} \sin\left(ln\sqrt{d_3} + sin^{10} d_0\right)\cos^2\left(d_3^3 - \left(\sqrt[3]{4.21 - d_1}\right)^2\right)\left(\sqrt[3]{d_2} - \cos\left((d_2 + \arctan 3.29) - d_0\right)\right) \quad (11)$$

Table 5. Evaluation of training and testing data statistically

Statistics	GEP Model	
	Training	Testing
R^2	0.99	0.95
Minimizing the absolute Percentage error	0.43	0.76
Root mean square error	0.31	0.69

Training and testing outcomes of the GEP model, along with the results of experimental studies, are depicted in Figure 5(a) and (b) respectively. These figures showcase the linear least square fit line, its computation, and the corresponding R^2 values for both datasets. During both the training and testing phases, these findings effectively forecast the elastic modulus values for polyethylene-CNT composites—Table 5 illustrates the R^2, MAPE, and RMSE values for both the training and testing sets. The EM values of polyethylene-Carbon Nanotube composites forecasts with the suggested GEP model. They are near the experimental values, as shown by the complete R^2, MAPE, and RMSE values.

Results indicate that the modeling technique suggested in this project is a replacement for the Deep Sensing Indentation technique to calculate the elastic modulus of PECNTs with a high correlation to the experimental ones.

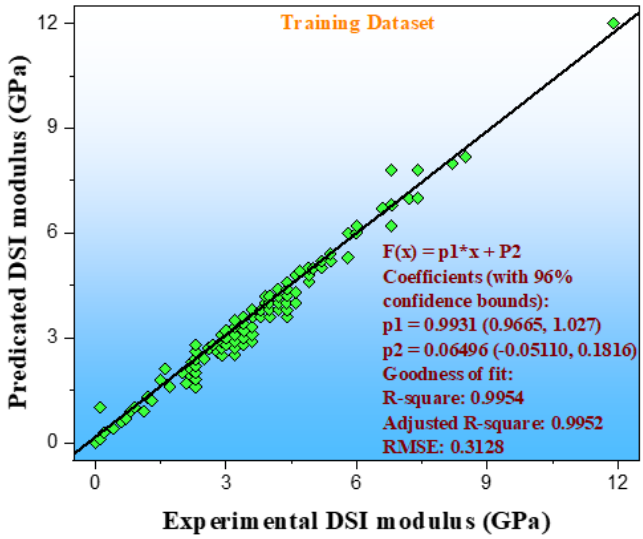

(a) During training

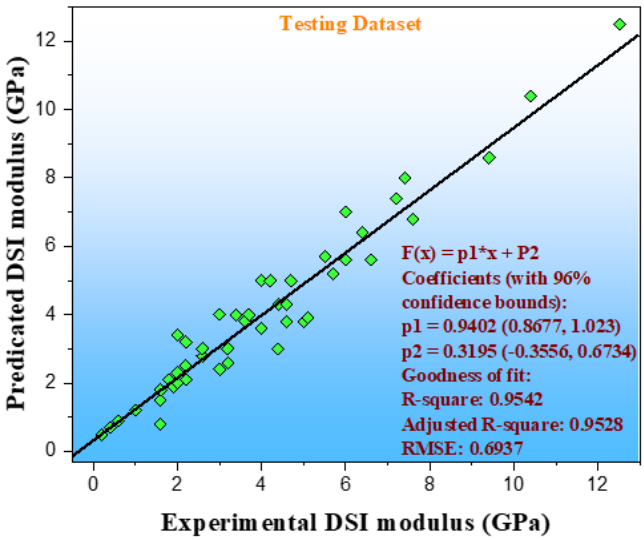

(b) During testing

Figure 5. Comparing the accuracy of the GEP model's predicted and observed values for elastic modules during (a) training and (b) testing

3.2 Statistical analysis of the AI model's performance

The statistical analysis of the performance of the artificial intelligence (AI) model, based on the data provided in Table 5, reveals outstanding results in both the training and testing sets. In the training set, the gene expression programming (GEP) model demonstrates an exceptionally high coefficient of determination (R^2) of 0.99, indicating outstanding ability to explain variability in the data used during training. Additionally, it minimizes the absolute percentage error to a low value of 0.43, signaling significant accuracy in predictions. The root mean square error (RMSE) in the training set is 0.31, demonstrating a well-fitted adjustment to the training data. These results underscore the GEP model's ability to adapt and fit well to the data used for training.

The R^2 achieves a high value of 0.95, indicating that the model effectively generalizes to unseen data during training. The absolute percentage error in the testing set is 0.76, slightly higher than the training set but still acceptable, suggesting consistent accuracy in predicting previously unused data. The RMSE in the testing set remains low, with a value of 0.69, emphasizing the model's ability to effectively forecast in new observations.

3.3 Compare AI predictions with traditional methods

In comparison to traditional methods used to simulate the behavior of polyethylene-carbon nanotube composites (PECNT), this research highlights the inherent complexity in such conventional approaches. The challenges associated with accuracy in simulating PECNT through traditional methods are addressed by the proposed method, employing a gene expression programming (GEP) model. The promising results of the GEP model in determining the elastic modulus (quasi-static) of PECNT suggest that it could overcome limitations observed in traditional methods, providing a more precise and effective alternative to tackle the complexity of these compounds. The application of GEP, with its evolutionary approach, could represent a significant advancement in the simulation of composite materials, surpassing the inherent limitations of traditional methods.

4. CONCLUSIONS

Since polyethylene-carbon nanotube composites (PECNTs) are complicated, accurately simulating their behavior is challenging to model. This research establishes a reliable method for determining the elastic modulus (quasi-static) of PECNTs over the relevant range. After applying the proposed method, the model's accuracy demonstrates that it can be a viable alternative to the DSI approach. As the connecting function, multiplication employs the GEP model, five sub-expression trees, thirty chromosomes, and a head size of ten. Based on the obtained data, it appears that GEP can serve as a viable alternative method for determining the EM values of PECNTs. The optimal values for R^2, minimizing absolute percentage error, and root mean square error in the training set are 0.99, 0.43, and 0.31, respectively. In the testing set, these values are 0.95, 0.76, and 0.69. The GEP model demonstrates its ability to provide accurate predictions for the EM values of PECNTs in the measured data, as evidenced by the favorable comparisons of R^2, MAPE, and root mean square error values.

REFERENCES

[1] Vinoth, A., Nirmal, K.N., Khedar, R., Datta, S. (2021). Optimizing the tribological properties of uhmwpe nanocomposites—An artificial intelligence based approach. In Trends in Mechanical and Biomedical Design: Select Proceedings of ICMechD 2019, Singapore, pp. 831-843. https://doi.org/10.1007/978-981-15-4488-0_70

[2] Vinoth, A., Datta, S. (2020). Design of the ultrahigh molecular weight polyethylene composites with multiple nanoparticles: An artificial intelligence approach. Journal of Composite Materials, 54(2): 179-192. https://doi.org/10.1177/0021998319859924

[3] You, J., Qin, W., Feng, H., Huang, R., Shangguan, J. (2015). Dynamic performance evaluation of computing system based on gene expression programming theory. International Journal of Innovative Computing, Information and Control, 11(5): 1725-1738. https://doi.org/10.24507/ijicic.11.05.1725

[4] You, J., Tian, S., Huang, R. (2015). Modeling the performance and determining the restart time of computing system based on gene expression programming theory. ICIC Express Letters. Part B, Applications: An International Journal of Research and Surveys, 6(6): 1607-1612.

[5] Madhan Kumar, A., Jayakumar, K. (2022). Mechanical and drilling characterization of biodegradable PLA particulate green composites. Journal of the Chinese Institute of Engineers, 45(5): 437-452. https://doi.org/10.1080/02533839.2022.2061602

[6] Luan, F., Cordeiro, M.N.D.S. (2012). Overview of QSAR modelling in rational drug design. Recent Trends on QSAR in the Pharmaceutical Perceptions. Bentham Science Publishers, 48: 194-241. https://doi.org/10.2174/978160805379711201010194

[7] Eghbalian, M., Ansari, R., Haghighi, S. (2023). A combined molecular dynamics-finite element multiscale modeling to analyze the mechanical properties of randomly dispersed, chemisorbed carbon nanotubes/polymer nanocomposites. Mechanics of Advanced Materials and Structures, 30(24): 5159-5175. https://doi.org/10.1080/15376494.2022.2114038

[8] Gürbüz, R., Sarac, B., Soprunyuk, V., Rezvan, A., Yüce, E., Schranz, W., Sarac, A.S. (2022). Carbon nanotube-polybutadiene-poly (ethylene oxide)-based composite fibers: Role of cryogenic treatment on intrinsic properties. Polymers for Advanced Technologies, 33(12): 3966-3976. https://doi.org/10.1002/pat.5828

[9] Yu, H., Bi, M., Zhang, C., Zhang, T., Zhang, X., Liu, H., Yao, S. (2022). Construction of high sulfur loading electrode with functional binder of polyacrylic acid polymer grafted with polyethylene glycol for lithium/sulfur batteries. International Journal of Energy Research, 46(15): 24565-24577. https://doi.org/10.1002/er.8601

[10] Alexander, R., Dinkar, A., Biswas, S., Dasgupta, K. (2021). Comparative study of different carbon reinforcements at different length scales on the properties of polyvinyl alcohol composites. Polymer Composites, 42(9): 4239-4252. https://doi.org/10.1002/pc.26142

[11] Mokoena, T.E., Mochane, M.J., Mokhena, T.C., Motloung, M.T., Sefadi, J.S. (2022). The effect of boron nitride, carbon nanotubes, and their synergy on the properties of LLDPE and LLDPE/wax blend. Polymer Engineering & Science, 62(10): 3180-3193. https://doi.org/10.1002/pen.26094

[12] Sahu, S.K., Rama Sreekanth, P.S. (2022). Mechanical, thermal and rheological properties of thermoplastic polymer nanocomposite reinforced with nanodiamond, carbon nanotube and graphite nanoplatelets. Advances in Materials and Processing Technologies, 8: 2086-2096. https://doi.org/10.1080/2374068X.2022.2034309

[13] Zhou, Z., Zhang, H., Qiu, J., Chen, P., Sun, W. (2022). Atomic insights into synergistic effect of pillared graphene by carbon nanotube on the mechanical properties of polymer nanocomposites. Nano Materials Science, 4(3): 235-243. https://doi.org/10.1016/j.nanoms.2021.07.002

[14] Pundhir, N., Pathak, H., Zafar, S. (2022). Crashworthiness performance of HDPE-kenaf and HDPE-CNT composite structures. Advances in Materials and Processing Technologies, 8: 1070-1088. https://doi.org/10.1080/2374068X.2021.1927644

[15] Abshirini, M., Saha, M.C., Altan, M.C., Liu, Y. (2022). 3D printed flexible microscaled porous conductive polymer nanocomposites for piezoresistive sensing

applications. Advanced Materials Technologies, 7(9): 2101555. https://doi.org/10.1002/admt.202101555
[16] Qin, Y., Xu, D., Zhang, S., Fan, X. (2022). Dynamic behavior of carbon nanotubes and basalt fiber reinforced coral sand cement mortar at high strain rates. Construction and Building Materials, 340: 127396. https://doi.org/10.1016/j.conbuildmat.2022.127396
[17] Bernardo, F., Bardon, J., Riche, A., Pelletier, H. (2022). Quasi-static and dynamic depth-sensing indentation measurements to characterize wear and mar resistance of coating–polymer systems. International Journal of Materials Research, 96(11): 1256-1261. https://doi.org/10.1515/ijmr-2005-0219
[18] Ilie, N. (2021). Microstructural dependence of mechanical properties and their relationship in modern resin-based composite materials. Journal of dentistry, 114: 103829. https://doi.org/10.1016/j.jdent.2021.103829
[19] Kowalewska, A., Herc, A.S., Bojda, J., Nowacka, M., Svyntkivska, M., Piorkowska, E., Szymański, W. (2021). Phase structure and properties of ternary polylactide/poly (Methyl methacrylate)/polysilsesquioxane blends. Polymers, 13(7): 1033. https://doi.org/10.3390/polym13071033
[20] Staudinger, U., Janke, A., Steinbach, C., Reuter, U., Ganß, M., Voigt, O. (2022). Influence of CNT length on dispersion, localization, and electrical percolation in a styrene-butadiene-based star block copolymer. Polymers, 14(13): 2715. https://doi.org/10.3390/polym14132715
[21] Ilie, N. (2021). Comparative analysis of static and viscoelastic mechanical behavior of different luting material categories after aging. Materials, 14(6): 1452. https://doi.org/10.3390/ma14061452
[22] Slouf, M., Strachota, B., Strachota, A., Gajdosova, V., Bertschova, V., Nohava, J. (2020). Macro-, micro-and nanomechanical characterization of crosslinked polymers with very broad range of mechanical properties. Polymers, 12(12): 2951. https://doi.org/10.3390/polym12122951
[23] Jayakumar, K., Mathew, J., Joseph, M.A. (2012). Analysis and prediction of end milling characteristics of Al-SiC p metal matrix composite using RSM and ANN. Journal for Manufacturing Science and Production, 12(2): 105-110. https://doi.org/10.1515/jmsp-2012-0009
[24] Pebdani, M.H., Sabetvand, R. (2022). Mechanical properties of carbon nanotube reinforced polyurethane matrix using computational method: A molecular dynamics study. Physica Scripta, 97(7): 075402. https://doi.org/10.1088/1402-4896/ac6cae
[25] Mazánková, V., Sťahel, P., Matoušková, P., Brablec, A., Čech, J., Prokeš, L., Trunec, D. (2020). Atmospheric pressure plasma polymerized 2-Ethyl-2-oxazoline based thin films for biomedical purposes. Polymers, 12(11): 2679. https://doi.org/10.3390/polym12112679
[26] Campos, J.M., del Río, B., Lorenzo, V., Ania, F., Barros-Timmons, A., Ribeiro, M.R. (2020). Improvement of viscoelastic, elastic and plastic properties of Poly (L-lactide)/Graphene Oxide-Graft-Poly (L-lactide) nanocomposites by modulation of grafted chain length. Composites Science and Technology, 199: 108350. https://doi.org/10.1016/j.compscitech.2020.108350
[27] Ania, F., Gómez-Fatou, M.A., Salavagione, H.J., Enrique-Jiménez, P., Quiles-Díaz, S., Flores, A. (2020). Creep behaviour of elastomeric nanocomposites by flat punch indentation: Influence of graphene modification and content. Composites Science and Technology, 198: 108311. https://doi.org/10.1016/j.compscitech.2020.108311
[28] Ovsik, M., Manas, M., Stanek, M., Dockal, A., Vanek, J., Mizera, A., Stoklasek, P. (2020). Polyamide surface layer nano-indentation and thermal properties modified by irradiation. Materials, 13(13): 2915. https://doi.org/10.3390/ma13132915
[29] Ovsík, M., Staněk, M., Dočkal, A., Fluxa, P. (2020). Local nano-mechanical properties of cross-linked polybutylene. Acta Polytechnica CTU Proceedings, 27: 112-115. https://doi.org/10.14311/APP.2020.27.0112
[30] Xu, L., Li, Z., Lu, H., Qi, X., Dong, Y., Dai, H., Ni, Q. (2022). Electrothermally-driven elongating-contracting film actuators based on two-way shape memory carbon nanotube/ethylene-vinyl acetate composites. Advanced Materials Technologies, 7(7): 2101229. https://doi.org/10.1002/admt.202101229
[31] Akar, A.O., Yildiz, U.H., Tirkes, S., Tayfun, U., Hacivelioglu, F. (2022). Influence of carbon nanotube inclusions to electrical, thermal, physical and mechanical behaviors of carbon-fiber-reinforced ABS composites. Carbon Letters, 32(4): 987-998. https://doi.org/10.1007/s42823-022-00332-y
[32] Ovsik, M., Manas, M., Stanek, M., Dockal, A., Mizera, A., Fluxa, P., Bednarik, M., Adamek, M. (2020). Nano-mechanical properties of surface layers of polyethylene modified by irradiation. Materials (Basel), 13(4): 929. https://doi.org/10.3390/ma13040929
[33] Sravanthi K., Rao B.N., Mahesh V. (2022). Effect of thermal ageing temperature and time on the mechanical properties of CNT/GFRP composites. AIP Conference Proceedings, 2393(1): 020206. https://doi.org/10.1063/5.0074294
[34] Lei, W.J., Gou, X.F. (2022). Effects of stone–wales defects of carbon nanotubes on the elastic properties of the carbon nanotube-polyethylene nanocomposite and its interface. Materials Research Express, 9(5): 055009. https://doi.org/10.1088/2053-1591/ac6ed0
[35] Kibrete, F., Trzepieciński, T., Gebremedhen, H.S., Woldemichael, D.E. (2023). Artificial intelligence in predicting mechanical properties of composite materials. Journal of Composites Science, 7(9): 364. https://doi.org/10.3390/jcs7090364
[36] Song, L., Wang, D., Liu, X., Yin, A., Long, Z. (2023). Prediction of mechanical properties of composite materials using multimodal fusion learning. Sensors and Actuators A: Physical, 358: 114433. https://doi.org/10.1016/j.sna.2023.114433
[37] Ilcheva, V., Boev, V., Zamfirova, G., Gaydarov, V., Lilova, V., Petkova, T. (2020). Transparent organic-inorganic hybrids obtained from covalently bonded ureasilicate monomers: Optical and mechanical properties. NATO Science for Peace and Security Series B: Physics and Biophysics, Dordrecht, pp. 59-65. https://doi.org/10.1007/978-94-024-2018-0_4
[38] Afsharhashemkhani, S., Jamal, M., Tavakolian, M. (2022). A molecular dynamics study on the mechanical properties of defective CNT/epoxy nanocomposites using static and dynamic deformation approaches. International Polymer Processing, 37(2): 176-190. https://doi.org/10.1515/ipp-2021-4182
[39] Sun, Z., Guo, F.L., Li, Y.Q., Hu, J.M., Liu, Q.X., Mo,

X.L., Huang, P., Fu, S.Y. (2022). Effects of carbon nanotube-polydopamine hybridization on the mechanical properties of short carbon fiber/polyetherimide composites. Composites Part B: Engineering, 236: 109848. https://doi.org/10.1016/j.compositesb.2022.109848

[40] Han, C.L., Zou, A.L., Wang, G.D., Li, N., Wang, M., Wei, L., Liu, X.L. (2022). The synergetic relation of flexural strain behaviors and electrical signals of carbon nanotube-based polymer laminates. European Physical Journal Plus, 137(4): 462. https://doi.org/10.1140/epjp/s13360-022-02641-7

[41] Dockal, A., Ovsik, M., Fluxa, P., Stanek, M., Senkerik, V. (2020). Implementation of natural fillers in polyethylene and the resulting mechanical properties. Materiali Tehnologije, 54(3): 341-343. https://doi.org/10.17222/mit.2019.154

[42] Mizera, A., Fiala, T., Manas, M., Stoklasek, P., Ovsik, M. (2020). Influence of injection moulding process parameters on high-density polyethylene surface hardness. Materials Science Forum, 994: 189-196. https://doi.org/10.4028/www.scientific.net/MSF.994.189

[43] Kaboglu, C., Ferik, E. (2022). Effects of carbon nanotubes on mechanical behavior of fiber reinforced composite under static loading. Materials Testing, 64(2): 294-302. https://doi.org/10.1515/mt-2021-2024

[44] Farajian, J., Alipanahi, A., Mahboubkhah, M. (2022). Analyses of mechanical properties and morphological behavior of additively manufactured ABS polymer, ABS/PBT blend, and ABS/PBT/CNT nanocomposite parts. Journal of Thermoplastic Composite Materials, 36(6): 2390-2411. https://doi.org/10.1177/08927057221092952

[45] Sťahel, P., Mazánková, V., Tomečková, K., Matoušková, P., Brablec, A., Prokeš, L., Jurmanová, J., Buršíková, V., Přibyl, R., Lehocký, M., Petr Humpolíček, P., Ozaltin, K., Trunec, D. (2019). Atmospheric pressure plasma polymerized oxazoline-based thin films-antibacterial properties and cytocompatibility performance. Polymers (Basel), 11(12): 2069. https://doi.org/10.3390/polym11122069

[46] Aly, K., Aboubakr, S.H., Bradford, P.D. (2022). One-step fabrication of bulk nanocomposites reinforced by carbon nanotube array fragments. Polymer Composites, 43(1): 94-110. https://doi.org/10.1002/pc.26359

[47] Triolo, C., Cardile, G., Pisano, M., Conzatti, L., Utzeri, R., Stagnaro, P., Patane, S., Santangelo, S., Moraci, N. (2021). High-density polyethylene/carbon nanotubes composites: Investigation on the factors responsible for the fracture formation under tensile loading. Journal of Polymer Research, 28(12): 454. https://doi.org/10.1007/s10965-021-02807-4

[48] Zhao, F., Chen, Y., Zhou, B., Li, Y., Xue, S. (2021). Modeling thermo-mechanical behaviors of carbon nanotube/polyurethane functionally graded shape memory polymer beam. Polymer Composites, 42(12): 6785-6800. https://doi.org/10.1002/pc.26340